Korean J. Chem. Eng., **31**(8), 1451-1459 (2014)
DOI: 10.1007/s11814-014-0085-4

pISSN: 0256-1115
eISSN: 1975-7220

Comparative removal of two textile dyes from aqueous solution by adsorption onto marine-source waste shell : Kinetic and isotherm studies

Mehdi Shirzad-Siboni*, Alireza Khataee,†, Fatemeh Vafaei**, and Sang Woo Joo***,†**

*Department of Environmental Health Engineering, School of Health, Guilan University of Medical Sciences, Rasht, Iran
**Research Laboratory of Advanced Water and Wastewater Treatment Processes,
Department of Applied Chemistry, Faculty of Chemistry, University of Tabriz, Tabriz, Iran
***School of Mechanical Engineering, Yeungnam University, Gyeongsan 712-749, Korea
(*Received 27 December 2013 • accepted 18 March 2014*)

Abstract−Scallop shell was used as a low-cost adsorbent for removal of two anionic textile dyes, Reactive Blue 19 (RB19) and Acid Cyanine 5 R (AC5R), from aqueous solutions. The adsorbent was characterized using inductively coupled plasma optical emission spectrometry (ICP-OES), X-ray diffraction (XRD), Fourier transform infrared spectroscopy (FT-IR) and scanning electron microscopy (SEM). The dye removal efficiency of scallop shell was determined as function of contact time, solution pH, initial dye concentration and adsorbent dosage. With increasing dye concentration, the adsorption of both dyes decreased, while it increased with increasing adsorbent dosage. Optimum removal of RB19 and AC5R was achieved at pH=6. Adsorption equilibrium data were well described by the Freundlich model. The maximum dye adsorption capacity of scallop shell as estimated from the Langmuir isotherm was 12.36 and 12.47 mg/g for RB19 and AC5R, respectively. The adsorption kinetic data showed excellent correlation with the pseudo-second-order model. It was concluded that scallop shell has a remarkable potential for the sorption of RB19 and AC5R and can be used for treatment of the dye contaminated wastewater.

Keywords: Scallop Shell, Kinetic Models, Adsorbent, Wastewater Treatment, Organic Dyes

INTRODUCTION

Textile, paper, cosmetic, leather, plastics, food, printing and pharmaceutical industries are the greatest consumers of organic dyes [1-3]. Large quantities of used dyes are wasted in the high volume of liquid effluents that discharge them in both terrestrial and aquatic ecosystems, creating serious environmental and health problems such as toxicity, carcinogenicity and mutagenicity effects in organisms [4-6]. Two classes of the most common dyes which are present in the effluent and increase risk factors for health are azo and reactive dyes group [7]. Cyanine 5R or Acid blue 113 as a diazo dye is widely used in the textile industry and has been recognized as a potential carcinogenic agent [8]. Due to its good water solubility and its strong interaction with fabrics, Reactive Blue 19 is also extensively consumed in coloring processes. However, it emits poisonous gases, especially at high temperatures [9]. Therefore, applying an efficient strategy to handle the colorful wastewater has always been considered. For cleanup purposes, various methods based on physical and chemical reactions, for example reverse osmosis [10], membrane filtration [11], chemical precipitation [12], electro-deposition [13], electro-coagulation [14], advanced oxidation process [15-17], and ion exchange process [18], have been developed. These approaches have several disadvantages, including the formation of hazardous by-products, the requirement for extensive equipment, chemicals, separation stage and high energy, which make them economically unsuitable [18,19]. Additionally, biodegradation of the majority of textile dyes, due to the stability and complexity of aromatic structure of dyes, is difficult or impossible. As a substitute, adsorption techniques have progressed as a simple, efficient, low cost process to eliminate dyes and organic matters from wastewater [20]. Although carbon-based materials are known as efficient adsorbents, the large-scale usage of them is restricted because of the relatively high cost of the preparation procedure (especially activated carbon) [3,5]. To compensate for this limitation, the effective removal of dyes using low-cost adsorbents including sawdust [21-24], agricultural residues [25], red mud [26], dolomite [27], fly ash [28], and oyster shell [29] has been reported. The common name of scallops refers to many species of marine bivalve mollusks that belong to the Pectinidae family. Since they have worldwide distribution in oceans and seas, scallop shells are produced as marine wastes. Besides, they are a component of food industry and restaurants wastes [30]. Hence, scallop shell can be economically used in adsorption of pollutants from wastewater. Yeom and Jung reported the adsorption ability of scallop shell in removal of phosphate [31].

In the present study, we investigated the potential of scallop shell in adsorption of two water-soluble textile anionic dyes (Reactive Blue 19 and Acid Cyanine 5 R) from aqueous solution. The characteristics of the scallop shell were analyzed by inductively coupled plasma optical emission spectrometry (ICP-OES), X-ray diffraction (XRD), Fourier transform spectrometry (FT-TR) and scanning electron microscopy (SEM). Also, its zero point charge (pHzpc) was determined. The effects of contact time, pH, initial dyes concentration and adsorbent dosage on the removal efficiency of the

†To whom correspondence should be addressed.
E-mail: a_khataee@tabrizu.ac.ir, ar_khataee@yahoo.com, swjoo@yu.ac.kr

dyes were studied. Adsorption isotherm and kinetic studies were undertaken to comprehend the adsorption mechanism and maximum adsorption capacity of scallop shell.

MATERIALS AND METHODS

1. Materials

All chemicals used were of analytical grades and solutions were prepared with deionized water (18 MΩcm) from a hydro-service reverse osmosis/ion exchange apparatus (Model LPRO-20, USA). Reactive Blue 19 and Acid Cyanine 5 R were purchased from Alvan Sabet Co., Iran. The chemical structure and absorption spectra of the dyes are given in Table 1 and Fig. 1, respectively.

2. Scallop Shell Sample

Scallop shell sample was collected from Caspian Sea beach in the city of Anzali in Guilan province of Iran, and then was washed with deionized water and dried at sunlight (Fig. 2(a)). It was then ground using a hammer mill for easy usage (Fig. 2(b)). The material obtained was dried in an electric furnace at 1,000 °C for 5 h, and sieved in the size range of 50 meshes ASTM (Fig. 2(c)).The scallop was characterized by inductively coupled plasma optical emission spectrometry (ICP-OES, Arcos EOP, Germany), Siemens X-ray diffractometer D5000 (Germany), Fourier transform spectrometers (FT-IR, Tensor 27, Bruker, Germany), and scanning electron microscope (SEM, Hitachi S-4200, Japan). Also, the zero point charge (pHzpc) of scallop shell powder was determined [30,32]. Adsorbent (0.2 g) was added to 40 mL of 0.1 M $NaNO_3$ solutions at various initial pH in the range of 2 to 11. The initial pH of solutions was adjusted by the addition of 0.1 M NaOH or HCl, and measured by pH meter (Metron, Switzerland). Afterward, the mixtures were shaken on a rotary shaker (KS-15, Edmund Buhler, Germany) at 170 rpm for 48 h at room temperature, and the final pH of each solution was measured at equilibrium.

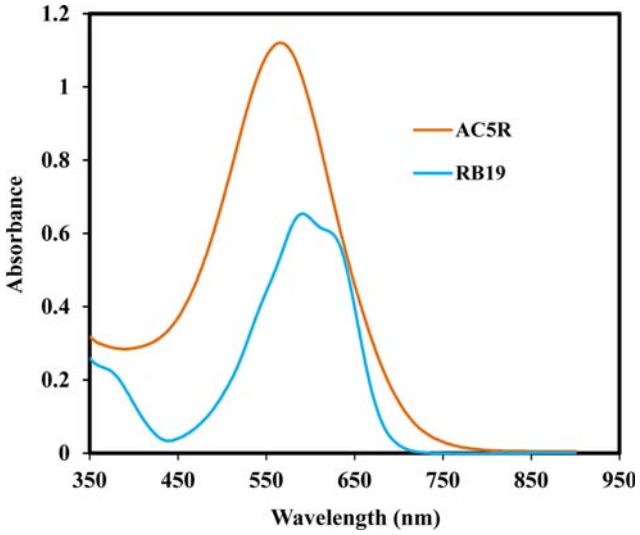

Fig. 1. The UV-Vis absorption spectra of the dyes.

3. Adsorption Experiments

The adsorption experiments were carried out in 250 mL Erlenmeyer flask containing 100 mL of dye solution and 1 g of scallop shell powder, while the mixtures were agitated at 150 rpm and room temperature (25±2 °C) for 120 min. Then, the samples were centri-

Table 1. The characteristics of the used dyes

Color index name	Reactive blue 19
Chemical structure	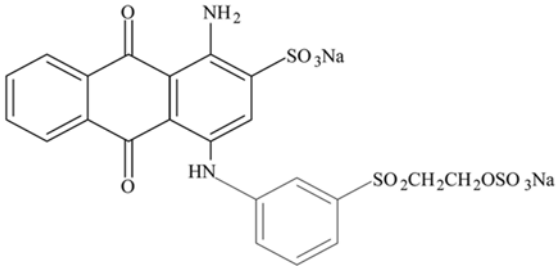
Synonym	Remazol brilliant blue R
Molecular formula	$C_{22}H_{16}O_{11}Nx\text{-}S_3Na_2$
λ_{max} (nm)	591
M_w (g/mol)	626.5
Color index name	Acid cyanine 5 R
Chemical structure	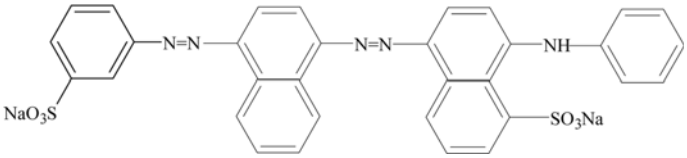
Synonym	Acid blue 113
Molecular formula	$C_{32}H_{21}N_5Na_2O_6S_2$
λ_{max} (nm)	566
M_w (g/mol)	681.65

Fig. 2. The images of scallop shell sample: (a) natural scallop shell, (b) ground sample using a hammer mill, (c) powdered sample in the size range of 50 meshes ASTM.

fuged (Sigma-301, Germany) at 4,000 rpm for 15 min to remove the adsorbent. The residual RB19 and AC5R dye concentration was determined by UV-Vis spectrophotometer (Hach-DR 5000, USA) at maximum absorbance wavelength of 591 and 566 nm, respectively [33]. To determine the effects of various parameters, the experiments were conducted by different adsorbent amounts of 0.4 to 30 g/L, initial dyes concentration of 20 to 500 mg/L and initial pH of 2 to 12. Each experiment was conducted in triplicate and mean values of data which were reported. Since standard deviations never exceeded ±1.5%, the error bars are not shown in the figures. The amount of dye adsorbed by the scallop shell and the dye removal efficiency was calculated through Eqs. (1) and (2) [34], respectively.

$$q_e = \frac{(C_0 - C)V}{M} \tag{1}$$

$$\text{Removal efficiency } (\%) = \frac{(C_0 - C)}{C_0} \times 100 \tag{2}$$

where, q_e is the adsorption capacity (mg/g) at equilibrium, C_0 and C are the initial and final dye concentration (mg/L), V is the volume of dye solution (L) and M is the total amount of scallop shell (g).

Adsorption kinetic experiments were carried out by agitating dye solutions (60, 100, 200 and 300 mg/L) containing 0.1 g/L of scallop shell powder for various contact times (5-120 min) at pH 6. The pseudo-first-order and pseudo-second-order models [35-37] were selected to find an efficient model for the best kinetically description of adsorption; the relevant equations are Eq. (3) and (4), respectively:

$$\log(q_e - q_t) = \log q_e - \frac{k_1}{2.303}t \tag{3}$$

$$\frac{t}{q_t} = \frac{1}{k_2 q_e^2} + \frac{1}{q_e}t \tag{4}$$

where q_e and q_t are the amounts of the dye adsorbed by scallop shell (mg/g) at the equilibrium and after a time t, respectively, and k_1 (1/min) and k_2 (g/(mg min) are the pseudo-first-order and pseudo-second-order rate constants, respectively.

To investigate the adsorption equilibrium isotherm, the experiments were performed with 100 mg/L initial concentration of dye using various adsorbent dosages (0.1-8 g/L) at pH 6 for 24 h. All experiments were repeated three times and the average values were reported. The commonly used isotherm equation, namely Langmuir and Freundlich [28,38], were applied to equilibrium data, the related equations are described by Eqs. (5) and (6), respectively:

$$q_e = \frac{K_L q_m C_e}{1 + K_L C_e} \tag{5}$$

$$\log q_e = \log K_F + \frac{1}{n}\log C_e \tag{6}$$

where q_m (mg/g) is maximum monolayer adsorption capacity, C_e is the sorbate concentration in solution at equilibrium (mg/L), K_L (L/mg) and K_F (mg/g) are the Langmuir and Freundlich constants, respectively, and n is the intensity of adsorption.

RESULTS AND DISCUSSION

1. Characterization of Scallop Shell

The main compositions of scallop shells were determined using ICP-EOS technique. Calcium (44,525.26 mg/kg), strontium (198.975 mg/kg), sodium (150.575 mg/kg), magnesium (32.2 mg/kg), potassium (9.175 mg/kg) and then barium (2.85 mg/kg) were the major components in the scallop shell sample according to dry weight. The XRD patterns recorded in Fig. 3 reveal the crystal structure of calcined scallop shell that mainly consist of $CaCO_3$ and CaO. Dur-

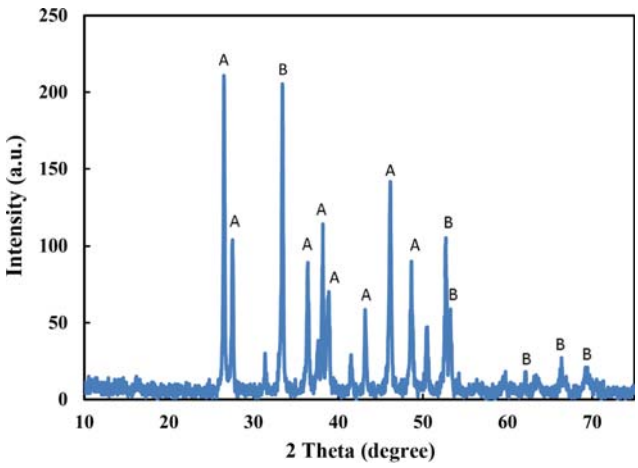

Fig. 3. XRD pattern of calcined scallop shell sample (A: $CaCO_3$ and B: CaO).

ing the calcination process due to the evolution of carbon dioxide, $CaCO_3$ converts to CaO and the rate of reaction depends on the temperature of the process, so that $CaCO_3$ totally transforms to CaO above 1,000 °C [39,40].

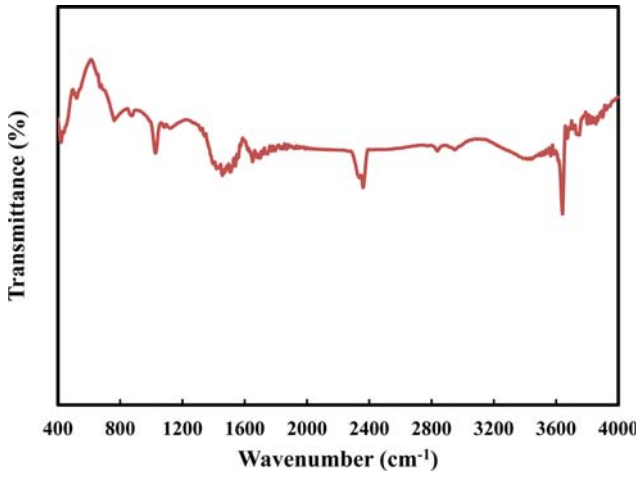

Fig. 4. FT-IR spectrum of calcined scallop shell sample.

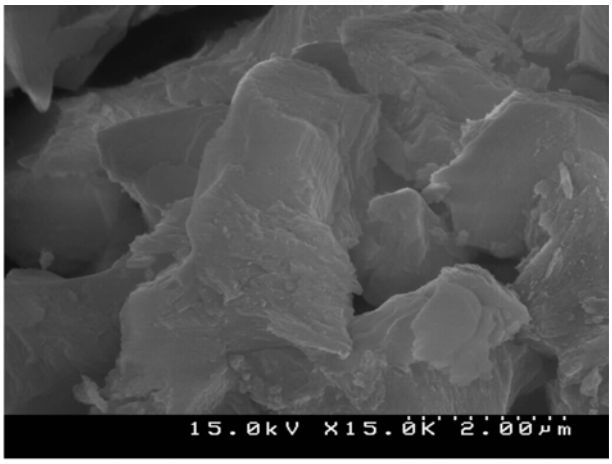

(a)

(b)

Fig. 5. SEM images of scallop shell samples: (a) before calcination, (b) after calcination of powdered sample in the size range of 50 meshes ASTM.

The adsorption reactions mostly occur on surface of the adsorbent, so the functional groups on the surface can play a significant role in the adsorption process. FT-IR analysis of calcined scallop shell shows the presence of active functional groups on the sample (Fig. 4). The observed peak at ~2,370 cm^{-1} can be assigned to the N-H group and a sharp peak at 3,645 cm^{-1} indicates the -OH stretching on the surface of scallop shell. The appearance of a broad peak around 1,500 cm^{-1} can be related to vibration peak of aromatic C=C and carbonyl C=O stretching. The peak at 1,040 cm^{-1} can be due to the six member cyclic ether group.

The microstructure and morphology of the scallop shells before and after calcination were characterized with SEM (Fig. 5). Fig. 5(a) shows the nonporous surface of the raw scallop shell. A porous structure, which is a good character for an adsorbent material, was observed on the surface of the calcined shell sample (Fig. 5(b)).

2. The Effect of Operational Parameters on the Dye Removal Efficiency

2-1. The Effect of Contact Time

The effect of contact time on the RB19 and AC5R removal by

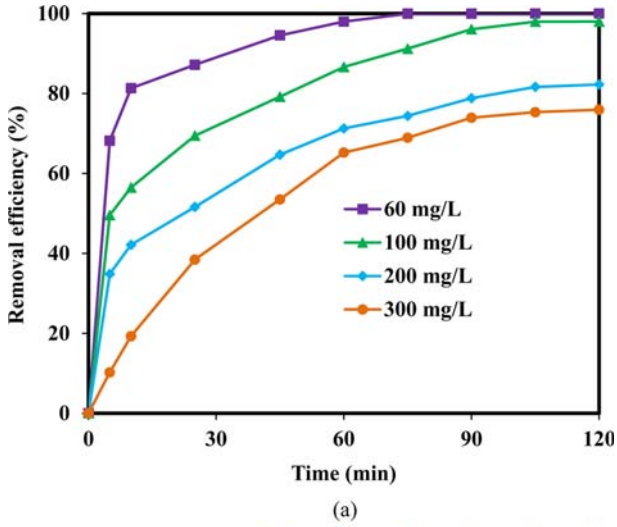

(a)

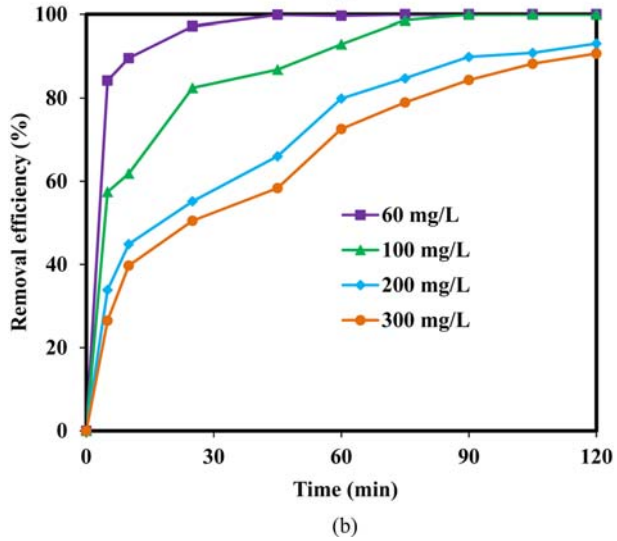

(b)

Fig. 6. The effect of contact time on the RB19 (a) and AC5R (b) removal by scallop shell: adsorbent dose=10 g/L, and pH=6.

scallop shell was studied by the variation of time from 5 to 120 min for different initial dye concentrations of 60, 100, 200 and 300 mg/L at pH of 6 and scallop shell dosage of 10 g/L (Fig. 6). As can be seen in Fig. 6, the rate of removal of two dyes at all concentrations is primarily rapid in the first stage of contact time, and then it gradually slows until reactions reach equilibrium at about 90 min. After that increase in the exposure time has a negligible effect on the efficiency of adsorption process. The rapid adsorption observed during the first steps of process is attributed to the abundance of free active sites on the scallop shell surface and easy availability of them for dye molecules. Subsequently, a decrease in the active sites due to their occupation by dye molecules and other hand repulsive forces among the adsorbed dye molecules on the scallop shell and bulk phase reduce the rapid of adsorption process [41,42]. The efficiency of dye removal for low concentrations of two dyes was greater than high concentration of them at the same reaction time. For example, the removal efficiency increased from 68.92% to 99.94% for RB19 and 78.95% to 99.99% for AC5R with an increase in the initial dyes concentration from 60 to 300 mg/L when the reaction times were 75 min. It seems evident that increasing the initial dye concentration because of the constant binding active sites on the adsorbent does not lead to augmented removal efficiency [34,43-45].

Despite these two dyes belonging to two different classes of synthetic dyes with dissimilar chemical structure, their removal efficiency by the same adsorbent was similar together. It is conceivable that same ion mode in RB19 and AC5R (i.e., two negative charges) plays an important role in the interaction between scallop shell and dyes.

2-2. The Effect of Solution pH and Determination of pH_{ZPC}

The effect of pH on the variation of RB19 and AC5R adsorption onto scallop shell was investigated for pH ranging between 2 and 12, and the results are in Fig. 7. As can be seen, various pHs do not have considerable influence on both dye adsorption. The removal efficiency of RB19 was increased from 91.07% to 97.97% by increasing pH from 2 to 6 then it was reduced when the initial pH was adjusted to the higher values and achieved the lowest with

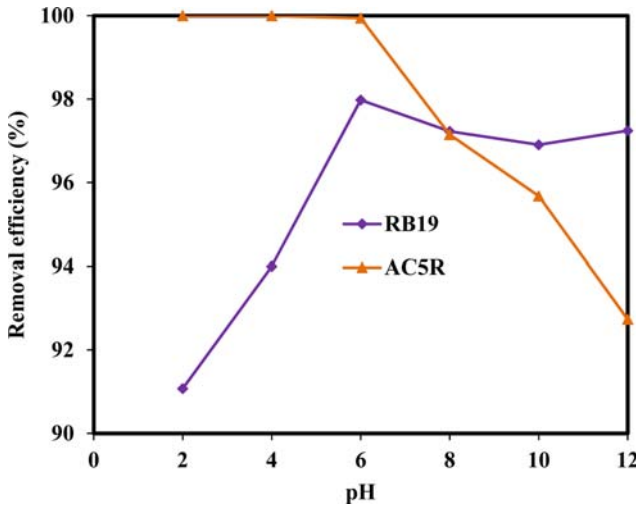

Fig. 7. The effect of pH on the removal of the dyes by scallop shell: initial dye concentration=100 mg/L, adsorbent dose=10 g/L, and contact time=120 min.

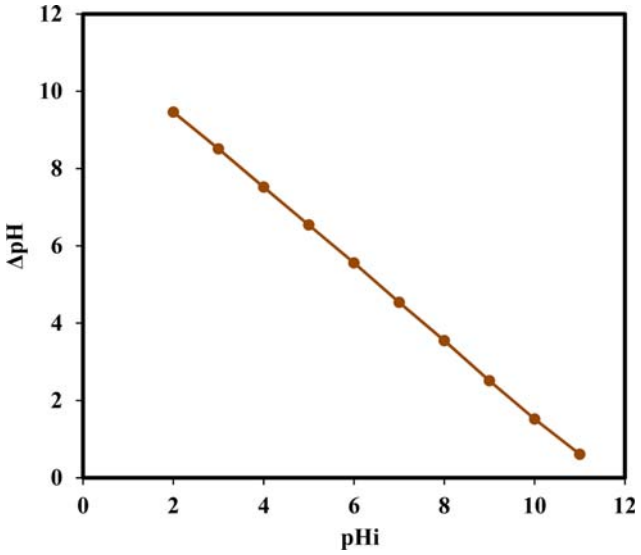

Fig. 8. Determination of the pH of point of zero charge (PZC).

97.24% at pH 12. The removal efficiency of AC5R was maximum (99.9%) at the pH range of 2-6. It was decreased with further increase in pH and reached to 92.73% at pH 12. To obtain information about the surface charge of the adsorbent, the pH of zero point charge (pH_{ZPC}) was determined. The plot of pH versus pHi of the solutions is illustrated in Fig. 8. It can be seen that pH_{ZPC} (the pH at which the net surface charge on scallop shell was zero (pH=0)) corresponds to a pH value around 11. This means that at pH values below 11 the scallop shell surface has a net positive charge, while at pH greater than 11 the surface has a net negative charge. Hence, the acidic pH facilitates the adsorption of the anionic dyes, RB19 and AC5R, onto scallop shell surface, as maximum removal of both dyes obtained at pH 6. This pH_{PZC} has a relatively high value compared to those reported in the literature for kaolin (pH_{pzc}=7) [46], and chitosan (pH_{pzc}=6.2) [47,48].

2-3. The Effect of Adsorbent Dosage

The influence of scallop shell dosage on the adsorption efficiency was investigated for ten various amounts in the range of 0.4-30 g/L (Fig. 9(a)). It is evident that the dye removal efficiency was increased from 69.29% to 99.99% for RB19 and 65.67% to 99.99 for AC5R by increasing the scallop shell dosage from 0.4 to 30 g/L. However, further increase in the adsorbent amounts did not affect the removal efficiency. Since there was no significant difference among dye removal in the values over 10 g/L, it was selected as the optimum dosage. The augmentation of decolonization efficiency with an increase in the scallop shell dosage was as a result of the presence of a high surface area, and consequently greater number of available sites for adsorption [21,49,50]. Nevertheless, the adsorption capacity decreased from 173.3 to 3.34 mg/g for RB19 and 164.2 to 3.34 mg/g for AC5R when the adsorbent dosage increased from 0.4 to 30 g/L (Fig. 9(b)). It can be explained by the reduction of the adsorption unsaturation sites that leads to comparatively less adsorption at large scallop shell dosages. Moreover, decreasing the effectiveness surface area for the sorption in the high adsorbent dosage could be due to partial covering or decrease in concentration gradient of adsorbent particles [4,34,51]. The results are consistent with previous literatures in which adsorption capacity decreased by increasing adsor-

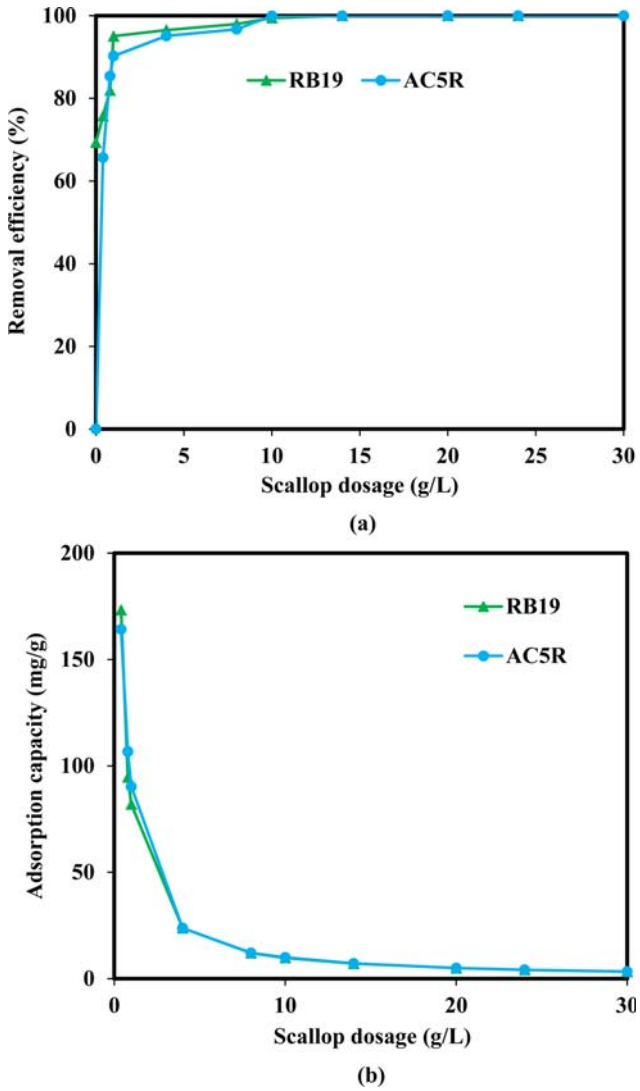

Fig. 9. The effect of adsorbent dose (a) and adsorption capacity (b) on the removal of the dyes by scallop shell: initial dye concentration=100 mg/L, contact time=120 min, and pH=6.

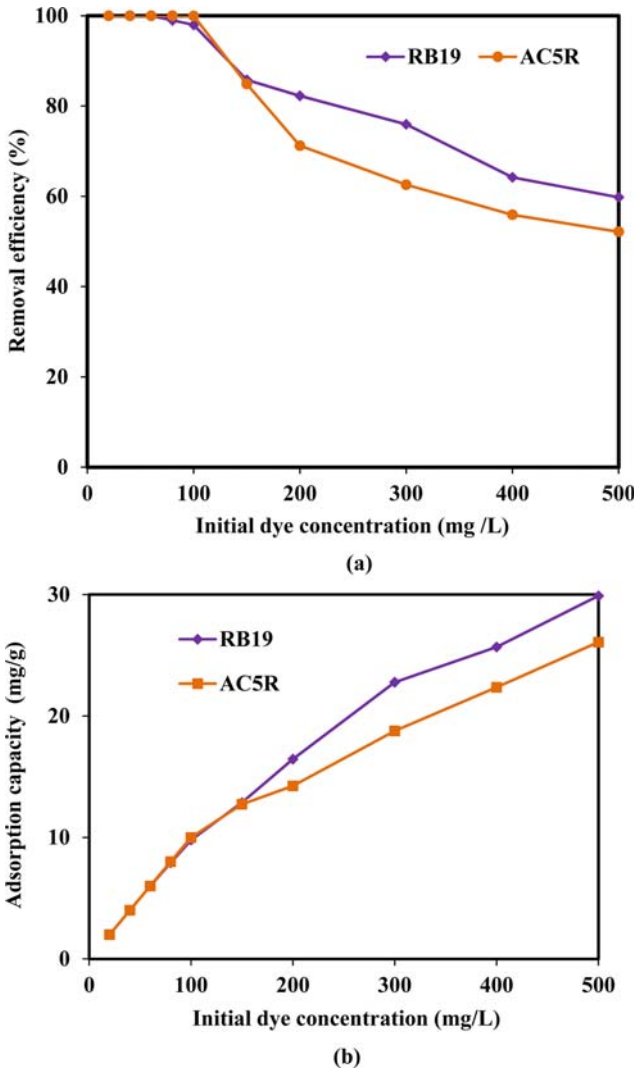

Fig. 10. The effect of initial dye concentration and adsorption capacity (b) on the dye removal efficiency by scallop shell: adsorbent dose=10 g/L, contact time=120 min, and pH=6.

bent dosage [38,52].

2-4. The Effect of Initial Dye Concentration

The initial dye concentration is one of the main factors controlling the adsorption capacity of dyes onto adsorbents by overcoming to the diffusive mass transfer barrier of between the dye molecules and sorbent. As can be seen from Fig. 10, although the removal efficiency because of the limited number of active sites declined along with increasing the initial dye concentration at above 100 mg/L, the adsorption capacity for both dyes exhibits the reverse trend. Exactly, when the initial dyes concentration were increased from 20 to 500 mg/L, the adsorption capacity of scallop shell was increased from 2 to 29.9 and 2 to 26.07 mg/g, and the dye removal efficiency was decreased from 99.99% to 59.78% and 99.99% to 52.15% for RB19 and AC5R, respectively. This may be because physical interaction between dye molecules and the scallop shell surface and overcoming to the diffusion barrier elevated with an increase in the dye concentration. Therefore, all the active sites would be more accessible for dye molecules at high concentration [34]. Similar observations were also reported for other dyes and different adsorbates by other adsorbents [53-55].

3. Kinetic and Isotherm Studies

The adsorption kinetic represents valuable data about efficiency of adsorption, reaction rate and pathways. Among kinetic models, pseudo-first-order and pseudo-second-order models are most commonly used to describe the adsorption. The pseudo-first-order and pseudo-second-order linear plots for the different initial concentrations of RB19 and AC5R are depicted in Figs. 11 and 12. The estimated kinetic parameters for both dyes are summarized in Table 2. The kinetic data of both dyes' adsorption had the best fitting (R^2=0.999 for both dyes) to pseudo-second-order model. Moreover, when the initial dye concentrations increased from 60 to 300 mg/L, the value of R^2 for pseudo-second-order model decreased and the value of q_e increased, indicating that adsorption data were in agreement with this model. The results are consistent with previous literatures in which adsorption kinetic of dyes by different adsorbent were fitted with pseudo-second-order model.

Adsorption isotherms show how adsorbate molecules distribute

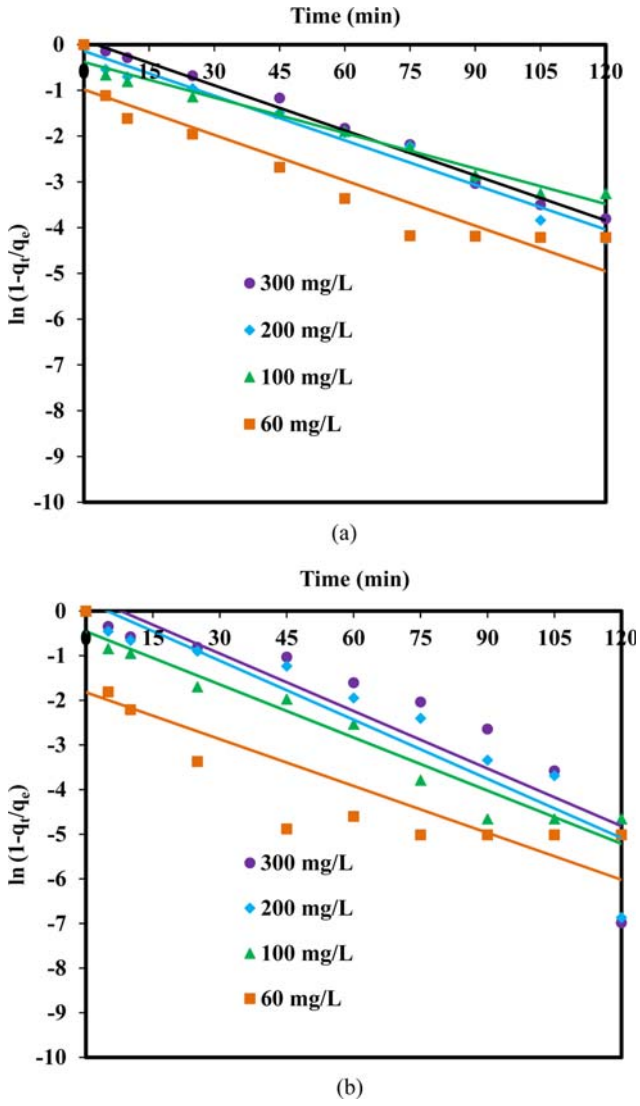

Fig. 11. The linear plots of pseudo-first-order models of RB19 (a) and AC5R (b) removal by scallop shell: adsorbent dose= 10 g/L, and pH=6.

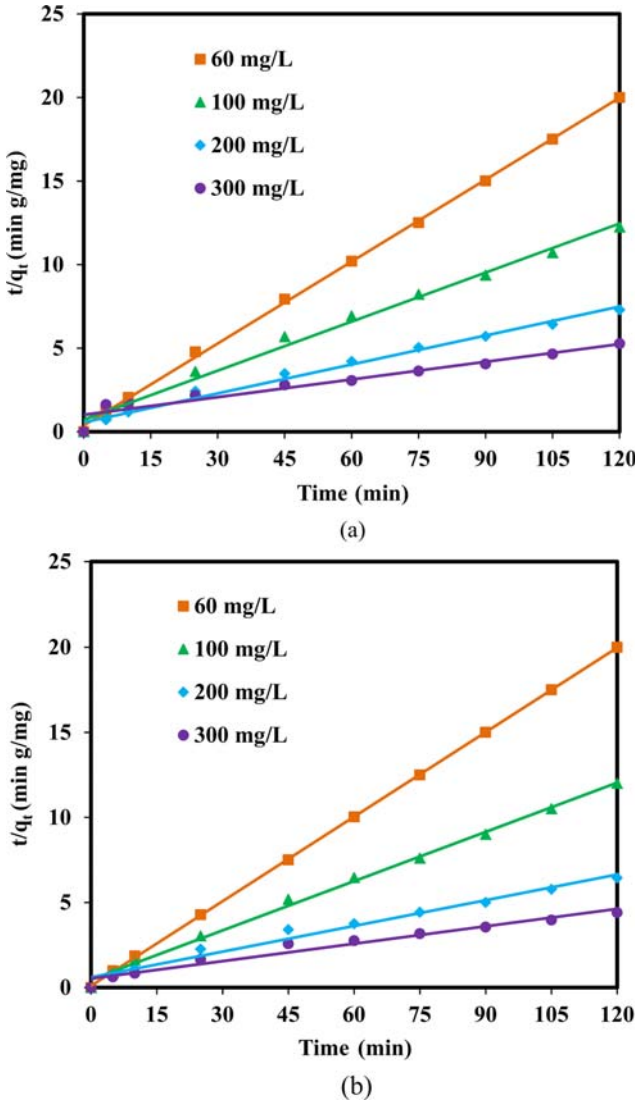

Fig. 12. The linear plots of pseudo-second-order models of RB19 (a) and AC5R (b) removal by scallop shell: adsorbent dose= 10 g/L, and pH=6.

Table 2. The calculated kinetic parameters for pseudo-first-order and pseudo-second-order models for removal of dyes by scallop shell

Reactive blue 19							
		Pseudo-first-order mode			Pseudo-second-order model		
C_0 (mg/L)	q_e (exp) (mg/g)	k_1 (1/min)	q_e (cal) (mg/g)	R^2	k_2 (g/mgmin)	q_e (cal) (mg/g)	R^2
60	5.99	0.033	6.09	0.883	0.07	6.14	0.999
100	9.79	0.025	10.19	0.972	0.013	10.19	0.991
200	16.45	0.032	16.69	0.975	0.005	17.54	0.986
300	22.78	0.032	23.3	0.991	0.001	28.57	0.933
Acid cyanine 5R							
		Pseudo-first-order mode			Pseudo-second-order model		
C_0 (mg/L)	q_e (exp) (mg/g)	k_1 (1/min)	q_e (cal) (mg/g)	R^2	k_2 (g/mgmin)	q_e (cal) (mg/g)	R^2
60	5.99	0.038	6.03	0.972	0.0227	6.06	0.999
100	9.99	0.039	10.09	0.952	0.019	10.42	0.996
200	18.62	0.0044	18.64	0.86	0.004	20.00	0.979
300	27.22	0.042	27.24	0.799	0.002	29.24	0.799

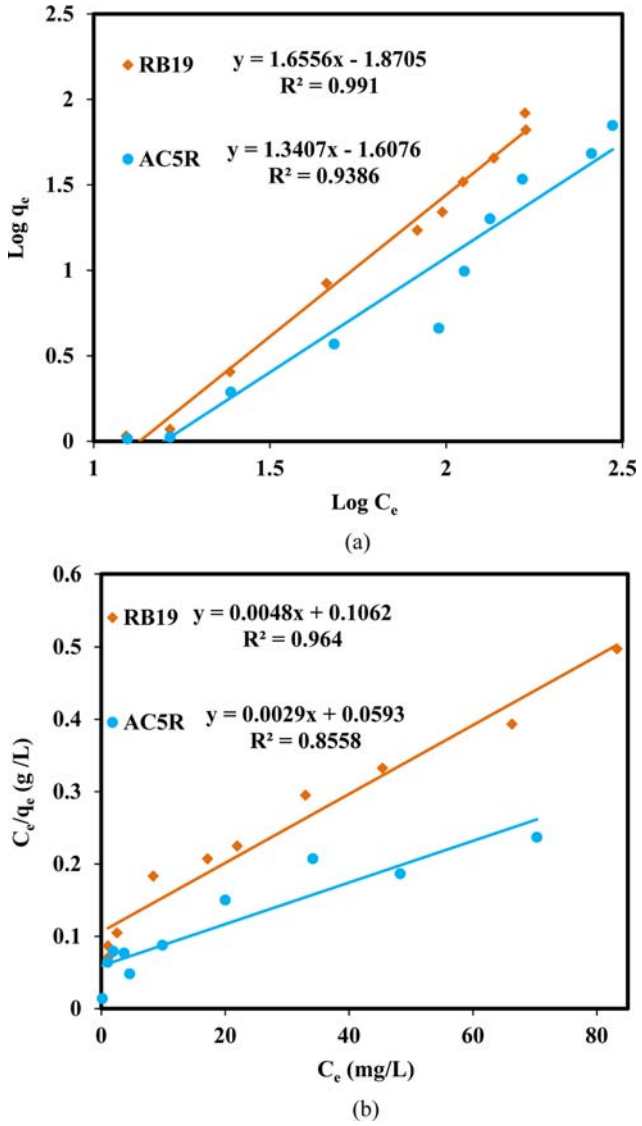

Fig. 13. The linear plots of (a) Freundlich isotherm and (b) Langmuir isotherm for the dye adsorption onto the scallop shell: initial dye concentrations=100 mg/L, adsorbent dose=0.1-8 g/L, contact time=24 h, pH=6.

between the liquid phase and the solid phase until reaching the equilibrium state and so are important in optimizing the adsorption process. In the present study, the Langmuir and Freundlich isotherms models were applied to the equilibrium data of RB19 and AC5R adsorption onto scallop shell. Therefore, Langmuir and Freundlich models were analyzed by plotting log (q_e) versus log (C_e) and C_e/q_e versus C_e, respectively (Fig. 13); and the estimated Langmuir and Freundlich constants and related correlation coefficients are given in Table 3. The high correlation coefficients (R^2=0.991 for RB19 and R^2=0.938 for AC5R) confirmed the applicability of the Freundlich model for the RB19 and AC5R adsorption process onto scallop shell. Thus, the adsorption of dyes onto scallop shell occurred as heterogeneous and multilayer phenomena. The high value of Freundlich constant (K_f=$mg^{1-1/n}$ $L^{1/n}$ g^{-1}) for RB19 can be related to the structural difference of these dyes. However, based on the Freundlich isotherm calculations the values of adsorption capacity of both dyes were similar to each other (12.36 and 12.47 mg/g for RB19 and AC5R, respectively).

The removal capacity of scallop shell is compared with the values reported for different adsorbents in Table 3. As the comparison shows, the scallop shell sample has effective higher adsorption capacity than others. Maximum adsorption capacity was obtained 250 and 500 mg/g at pH of 6 for RB19 and AC5R, respectively. Based on the obtained results, the scallop shell can be employed as an efficient and low-cost adsorbent for the removal of dyes.

CONCLUSIONS

The present study confirmed that scallop shell could be used as a cheap and available adsorbent for removal of the dyes from contaminated water. The decolorization efficiency depended on experimental parameters like contact time, initial dye concentration, the amount of scallop shell and pH. The removal efficiency at optimum pH 6 was found to increase with increase in contact time and adsorption dosage, but to decrease with increase in initial dye concentration. Analysis of the scallop shell by ICP-OES, XRD, FT-IR, and SEM revealed crystal structure, functional groups and porous surface contributed in the dye adsorption. Pseudo-second-order model described the adsorption kinetics of dyes onto scallop shell better than first one. The high value of correlation coefficient for the Freundlich isotherm pointed out that adsorption occurred on heterogeneous and multilayer surfaces. According to the results from the Freundlich model, the equilibrium adsorption capacity for RB19 and AC5R was 12.36 and 12.47 mg/g, respectively.

ACKNOWLEDGEMENTS

The authors thank the Guilan and Iran University of Medical Sciences and University of Tabriz, Iran for all of the support. We are

Table 3. The comparison of isotherm constants for the adsorption of dyes

	Freundlich constants				Langmuir constants			
Adsorbent	Dye name	K_F (mg/g)	n	R^2	q_m (mg/g)	K_L (L/mg)	R^2	Reference
Modified bentonite	RB19	6.31	2.137	0.991	2.15	6.61	0.997	[56]
Furnace slag	RB19	3.00	1.85	0.981	74.40	0.011	0.995	[57]
Activated carbon	AC5R	0.0001	2.06	0.8572	71.19	0.93	0.9927	[58]
Rubber tire	AC5R	75.3	1.79	0.9617	9.2	3.95	0.9968	[58]
Scallop shell	RB19	74.13	6.06	0.991	250	0.038	0.962	Present study
Scallop shell	AC5R	40.45	0.75	0.938	500	0.034	0.855	Present study

thankful to Mrs. Sevda Fallah for her assistance. This work is funded by the Grant 2011-0014246 of the National Research Foundation of Korea.

REFERENCES

1. A. R. Khataee, V. Vatanpour and A. R. Amani Ghadim, *J. Hazard. Mater.*, **161**, 1225 (2009).
2. S. Chakraborty, S. Chowdhury and P. Das Saha, *Carbohydr. Polym.*, **86**, 1533 (2011).
3. S. Chakraborty, S. Chowdhury and P. Saha, *Korean J. Chem. Eng.*, **29**, 1567 (2012).
4. A. R. Khataee, F. Vafaei and M. Jannatkhah, *Int. Biodeterior. Biodegrad.*, **83**, 33 (2013).
5. S. Chakraborty, S. De, S. DasGupta and J. K. Basu, *Chemosphere*., **58**, 1079 (2005).
6. S. Chowdhury, S. Chakraborty and P. Saha, *Colloids Surf.. B*., **84**, 520 (2011).
7. S. Yang, X. Yang, X. Shao, R. Niu and L. Wang, *J. Hazard. Mater.*, **186**, 659 (2011).
8. P. Mehta, R. Mehta, M. Suranaa and B. V. Kabrab, *J. Curr. Chem. Pharma. Sci.*, **1**, 28 (2011).
9. S. Song, J. Yao, Z. He, J. Qiu and J. Chen, *J. Hazard. Mater.*, **152**, 204 (2008).
10. S. K. Nataraj, K. M. Hosamani and T. M. Aminabhavi, *Desalination*., **249**, 12 (2009).
11. J. Wu, M. Eitemand and S. Law, *J. Environ. Eng.*, **124**, 272 (1998).
12. M.-X. Zhu, L. Lee, H.-H. Wang and Z. Wang, *J. Hazard. Mater.*, **149**, 735 (2007).
13. B. O'Regan and D. T. Schwartz, *Chem. Mater.*, **7**, 1349 (1995).
14. I. A. Sengila and M. Ozacarb, *J. Hazard. Mater.*, **161**, 1369 (2009).
15. M. Shirzad-Siboni, M. Samarghandi, J.-K. Yang and S.-M. Lee, *J. Adv. Oxid. Technol.*, **14**, 302 (2011).
16. N. Daneshvar, M. H. Rasoulifard, A. R. Khataee and F. Hosseinzadeh, *J. Hazard. Mater.*, **143**, 95 (2007).
17. N. Daneshvar, D. Salari and A. R. Khataee, *J. Photochem. Photobiol., A*., **157**, 111 (2003).
18. S. Raghu and C. Ahmed Basha, *J. Hazard. Mater.*, **149**, 324 (2007).
19. P. D. Saha, S. Chowdhury, M. Mondal and K. Sinha, *Sep. Sci. Technol.*, **47**, 112 (2011).
20. Z. Eren and F. N. Acar, *Desalination*, **194**, 1 (2006).
21. V. K. Garg, R. Gupta, A. Bala Yadav and R. Kumar, *Bioresour. Technol.*, **89**, 121 (2003).
22. P. K. Malik, *J. Hazard. Mater.*, **113**, 81 (2004).
23. F. Ferrero, *J. Hazard. Mater.*, **142**, 144 (2007).
24. O. Mahmut and S. I. Ayhan, *Process Biochem.*, **40**, 565 (2005).
25. P. Nigam, G. Armour, I. M. Banat, D. Singh and R. Marchant, *Bioresour. Technol.*, **72**, 219 (2000).
26. S. Wang, Y. Boyjoo, A. Choueib and Z. H. Zhu, *Water Res.*, **39**, 129 (2005).
27. G. M. Walker, L. Hansen, J. A. Hanna and S. J. Allen, *Water Res.*, **37**, 2081 (2003).
28. Z. Eren and F. N. Acar, *J. Hazard. Mater.*, **143**, 226 (2007).
29. Z. Qiu-yue, Y. Ping, W. Yan and J. Lei, *Technol. Develop. Chem. Ind.*, 06 (2010).
30. M. Shirzad-Siboni, A. Khataee and S. W. Joo, *J. Ind. Eng. Chem.* 20 (2014).
31. S. H. Yeom and K.-Y. Jung, *J. Ind. Eng. Chem.*, **15**, 40 (2009).
32. N. Daneshvar, D. Salari, A. Niaei, M. H. Rasoulifard and A. R. Khataee, *J. Environ. Sci. Heal. A.*, **40**, 1605 (2005).
33. APHA; AWWA; WEF. Standard Methods for the Examination of Water and Wastewater, 20th Ed., American Public Health Association, American Water Works Association, and Water Environment Federation, Washington, DC, USA (2000).
34. S. Gupta and B. V. Babu, *Chem. Eng. J.*, **150**, 352 (2009).
35. S. Azizian, *J. Colloid Interface Sci.*, **276**, 47 (2004).
36. M. R. Samarghandi, S. Azizian, M. Shirzad-Siboni, S. J. Jafari and S. Rahimi, *Iran. J. Environ. Heal. Sci. Eng.*, **8**, 181 (2011).
37. M. Ghaedi, J. Tashkhourian, A. Pebdani, B. Sadeghian and F. Ana, *Korean J. Chem. Eng.*, **28**, 2255 (2011).
38. M. Shirzad-Siboni, M. R. Samarghandi, S. Azizian, W. G. Kim and S. M. Lee, *Environ. Eng. Res.*, **16**, 1 (2011).
39. M. Mohamed, S. Yusup and S. Maitra, *J. Eng. Sci. Technol.*, **7**, 1 (2012).
40. S. Castilho, A. Kiennemann, M. F. Costa Pereira and A. P. Soares Dias, *Chem. Eng. J.*, **226**, 146 (2013).
41. G. V. Kumar, P. Ramalingam, M. Kim, C. Yoo and M. D. Kumar, *Korean J. Chem. Eng.*, **27**, 1469 (2010).
42. P. Kumar, S. Ramalingam and K. Sathishkumar, *Korean J. Chem. Eng.*, **28**, 149 (2011).
43. E. Daneshvar, M. Kousha, M. S. Sohrabi, A. Khataee and A. Converti, *Chem. Eng. J.*, **195-196**, 297 (2012).
44. N. R. Bishnoi, R. Kumar, S. Kumar and S. Rani, *J. Hazard. Mater.*, **145**, 142 (2007).
45. M. Mondal, R. Singh, A. Kumar and B. Prasad, *Korean J. Chem. Eng.*, **28**, 1386 (2011).
46. B. K. Nandi, A. Goswami and M. K. Purkait, *Appl. Calay. Sci.*, **42**, 583 (2009).
47. W. S. Wan Ngah, L. C. Teong and M. A. K. M. Hanafiah, *Carbohydr. Polym.*, **83**, 1446 (2011).
48. S. Chatterjee, S. Chatterjee, B. P. Chatterjee and A. K. Guha, *Colloids Surf. A*., **299**, 146 (2007).
49. J. Barron-Zambrano, A. Szygula, M. Ruiz, A. M. Sastre and E. Guibal, *J. Environ. Manage.*, **91**, 2669 (2010).
50. K. Bellir, I. S. Bouziane, Z. Boutamine, M. B. Lehocine and A. H. Meniai, *Energy Procedia*., **18**, 924 (2012).
51. M. Kousha, E. Daneshvar, A. R. Esmaeli, M. Jokar and A. R. Khataee, *Int. Biodeterior. Biodegrad.*, **69**, 97 (2012).
52. L. Wang, J. Zhang, R. Zhao, C. Li, Y. Li and C. Zhang, *Desalination*., **254**, 68 (2010).
53. M. Toor and B. Jin, *Chem. Eng. J.*, **187**, 79 (2012).
54. O. Tunc, H. Tanaci and Z. Aksu, *J. Hazard. Mater.*, **163**, 187 (2009).
55. L. Li, S. Liu and T. Zhu, *J. Environ. Sci.*, **22**, 1273 (2010).
56. Ö. Gök, A. S. Özcan and A. Özcan, *Appl. Surf. Sci.*, **256**, 5439 (2010).
57. Y. Xue, H. Hou and S. Zhu, *Chem. Eng. J.*, **147**, 272 (2009).
58. V. K. Gupta, B. Gupta, A. Rastogi, S. Agarwal and A. Nayak, *J. Hazard. Mater.*, **186**, 891 (2011).